Article

Not peer-reviewed version

ML-Assisted Prediction of In-Cylinder Pressures of Spark Ignition Engines

Yu Zhang , Qianbing Xu , Xinfeng Zhang *

Posted Date: 16 March 2026

doi: 10.20944/preprints202603.1219.v1

Keywords: gasoline engine; pressure reconstruction; machine learning; combustion diagnosis; spark advance angle

doi:10.20944/preprints202603.1219.v1

Article

ML-Assisted Prediction of In-Cylinder Pressures of Spark Ignition Engines

Yu Zhang [1], Qianbing Xu [1] and Xinfeng Zhang [2,*]

[1] Hangzhou City University College of Engineering, Hangzhou 310015, China
[2] Hangzhou City University School of Information and Electrical Engineering, Hangzhou 310015, China
* Correspondence: zxf@hzcu.edu.cn

Abstract

In-cylinder pressure is a critical parameter for assessing the combustion process and per-formance of spark ignition internal combustion engines. However, obtaining measured in-cylinder pressure data across the full operating range, particularly at various spark advance angles (SA), is costly and technically demanding, limiting its widespread application in engineering practice. This study proposes two artificial neural network (ANN) based in-cylinder pressure reconstruction methods utilizing in-cylinder pressure and heat release rate data from a three-cylinder motorcycle gasoline engine under varying spark advance angle conditions, aiming to achieve cost-effective, high-precision pressure prediction through machine learning technology. Both pressure reconstruction methods employ crank angle and spark advance angle as input features. Method 1 (ANN-P) directly predicts the in-cylinder pressure curve, achieving a coefficient of determination R^2 exceeding 0.99 on both training and validation sets with a root mean square error (RMSE) below 0.13 bar, accurately reproducing the pressure evolution throughout the compression, combustion, and expansion processes while achieving high-precision prediction of indicated mean effective pressure (IMEP). Method 2 (ANN-HRR) adopts an indirect strategy of "predicting heat release rate followed by integration to reconstruct pressure." This method first derives the apparent heat release rate (HRR) from measured in-cylinder pressure data, trains a machine learning algorithm with HRR data to predict the target operating condition's HRR curve, then reconstructs in-cylinder pressure through integral inversion based on a single-zone thermodynamic model, thereby avoiding error amplification caused by differential operations. This approach demonstrates superior performance in predicting combustion characteristic points (CA10, CA50). The results demonstrate that both methods accurately capture the influence of spark timing on combustion phasing and peak pressure. Method 1 achieves high accuracy in predicted pressure curves but exhibits lower accuracy in capturing combustion characteristics; Method 2 effectively compensates for the limitations of Method 1 in characterizing combustion features through heat release rate curve prediction. This study provides an economical and efficient technical approach for gasoline engine combustion diagnosis, performance calibration, and control optimization.

Keywords: gasoline engine; pressure reconstruction; machine learning; combustion diagnosis; spark advance angle

---

1. Introduction

Internal combustion engines, as core power units in transportation, engineering machinery, and distributed power generation, will continue to play an irreplaceable role in the global energy transition process [1,2]. Facing increasingly stringent carbon emission regulations and energy efficiency standards, achieving efficient and clean combustion in internal combustion engines has become a core research topic in power engineering [3]. Cylinder pressure, as the most direct physical parameter characterizing the combustion process, contains critical combustion characteristic information in its time-domain evolution, including combustion onset, combustion center, peak pressure location, and combustion duration [4]. Accurate acquisition and in-depth analysis of in-cylinder pressure data provide irreplaceable guidance for combustion diagnosis, thermal efficiency optimization, knock detection, and emission control [5,6].

In spark-ignition internal combustion engines, spark advance angle is a key control parameter that regulates combustion phasing and affects thermal efficiency and pollutant formation. Research indicates that when ignition timing deviates from the optimal value by 2°CA, indicated thermal efficiency decreases by approximately 1% [7]. However, determining the optimal spark advance angle requires systematic bench calibration experiments across various speeds, loads, intake temperatures, and air-fuel ratios [8]. With the widespread adoption of advanced technologies such as variable valve timing, lean combustion, exhaust gas recirculation, and pre-chamber ignition, the dimensionality of engine control parameters has increased dramatically, and traditional point-by-point calibration methods face severe challenges from the "curse of dimensionality" [9,10]. Traditional in-cylinder pressure acquisition relies on direct measurement using high-precision piezoelectric pressure sensors, but this approach faces numerous challenges: sensors are costly and installation requires precision machining of the cylinder head; sensors suffer from thermal drift and signal distortion in high-temperature, high-pressure environments; full-range calibration experiments require lengthy cycles and substantial resource consumption, making it difficult to meet rapid development iteration demands [11,12]. In numerical simulation, zero-dimensional/quasi-dimensional thermodynamic models are established based on conservation equations and Wiebe functions with clear physical meaning, but key parameter calibration still depends on substantial experimental data and cannot accurately describe complex turbulent flame propagation processes [13]. Three-dimensional CFD methods can provide detailed information on in-cylinder flow field and combustion evolution, but computational costs for a single operating point reach tens to hundreds of CPU hours, making them impractical for real-time prediction and large-scale operating condition scanning [14,15].

In recent years, the rapid development of machine learning technology has opened new avenues for internal combustion engine combustion modeling. Aliramezani et al. [16] systematically reviewed machine learning applications in engine modeling, diagnosis, optimization, and control, noting that data-driven methods show enormous potential in handling high-dimensional nonlinear problems. Ihme et al. [17] comprehensively summarized the principles, progress, and prospects of combustion machine learning, providing important guidance for research in this field. Artificial neural networks, with their powerful nonlinear mapping capability and self-learning characteristics, have become one of the most widely applied algorithms in internal combustion engine performance prediction [18]. Building on this foundation, Solmaz et al. [19] compared the performance of ANN and fuzzy logic in cylinder pressure prediction for spark-ignition engines, finding that ANN models demonstrate higher accuracy and robustness than fuzzy logic in reconstructing in-cylinder pressure curves with crank angle resolution and determining optimal ignition advance angle under various speeds and ignition timings. In cylinder pressure prediction, Yao et al. [20] constructed a high-precision cylinder pressure prediction model based on SSA-BiLSTM, significantly improving prediction stability under transient operating conditions. Zhang et al. [21] proposed a deep learning reconstruction method based on multi-source vibration information fusion, achieving high-precision cylinder pressure curve estimation under sensor less conditions. Furthermore, physics-informed neural networks enhance model generalization and physical consistency by embedding physical laws into loss functions [22,23]. Omoyele et al. [24] combined automatic machine learning with genetic algorithms for rapid engine design optimization, significantly reducing development cycles. Gaussian process regression, support vector machines, and extreme gradient boosting methods have also been successfully applied in engine calibration and emission prediction [25,26]. Addressing the full-cycle cylinder pressure reconstruction problem under unmeasured conditions, Liu et al. [27] recently proposed a machine learning-assisted framework that, by comparing direct pressure prediction, indirect prediction based on HRR integration, and hybrid strategies, found that although direct prediction can better fit pressure trajectories, it tends to underestimate combustion characteristics. A hybrid

 doi:10.20944/preprints202603.1219.v1

strategy combining non-combustion segment pressure prediction with combustion segment HRR prediction can achieve high-fidelity reconstruction of cylinder pressure curves under unmeasured altitude conditions while ensuring physical consistency. Despite the rapid development of machine learning in engine modeling, numerous challenges remain. First, existing research is mostly limited to single-point prediction, lacking full-cycle cylinder pressure reconstruction critical for combustion diagnosis; second, insufficient coupling of physical constraints leads to poor physical consistency under varying operating conditions; third, research on dynamic response of spark advance angle is limited, restricting model applications in control optimization.

Addressing these challenges, this paper focuses on a naturally aspirated three-cylinder gasoline motorcycle engine and proposes a machine learning-based in-cylinder pressure reconstruction framework aimed at achieving high-precision pressure prediction under unmeasured spark advance angle conditions. The study constructs and systematically compares two reconstruction strategies: Method 1 (ANN-P) takes crank angle and spark advance angle as input features and directly establishes nonlinear mapping relationships between input variables and in-cylinder pressure; Method 2 (ANN-HRR) introduces physical constraints by first using machine learning to predict the HRR curve of the target operating condition, then reconstructing in-cylinder pressure through integral inversion based on the first law of thermodynamics. Given that combustion is a continuous physicochemical process, obtaining complete crank angle-resolved continuous cylinder pressure curves is crucial for accurately extracting key characteristic parameters such as combustion onset, peak pressure location, and combustion duration. Through comparing the performance differences of the two methods in pressure curves, heat release rate, IMEP, and combustion characteristic point prediction, the study provides in-depth analysis of their respective advantages and limitations, offering theoretical basis and technical guidance for engineering applications of machine learning technology in internal combustion engine combustion analysis.

2. Data Collection and Machine Learning Modeling

To verify the feasibility of reconstructing in-cylinder pressure based on machine learning (ML), this study focuses on training and predicting in-cylinder pressure variations under different spark advance angle conditions. The experimental data originates from a naturally aspirated, water-cooled, four-stroke, three-cylinder motorcycle gasoline engine operating under steady-state conditions, with a displacement of 675 mL and a compression ratio of 11.5. On the test bench, data including torque, power, and fuel consumption rate were measured across engine speeds of 2000-11500 rpm and throttle openings of 0-100%, with the test process illustrated in Figure 1(a). A one-dimensional thermodynamic calculation model of the gasoline engine was established using GT-Power software, as shown in Figure 1(b), and calibrated according to experimental data. Within the range of -34°CA to -6°CA, eight discrete spark advance angle conditions were selected with an increment of 4°CA, with other parameters held constant. In-cylinder pressure data and heat release rate data were obtained using GT-Power software. The crankshaft angle range corresponding to each condition was -73°CA to 646°CA with a resolution of 0.1°CA. IMEP and torque data for the gasoline engine were obtained by performing integration calculations on the in-cylinder pressure data. Comparison of these data with measured values showed torque errors below 5% under all conditions, as shown in Figure 2, indicating that the GT-Power model possesses high predictive capability across all test conditions.

 doi:10.20944/preprints202603.1219.v1

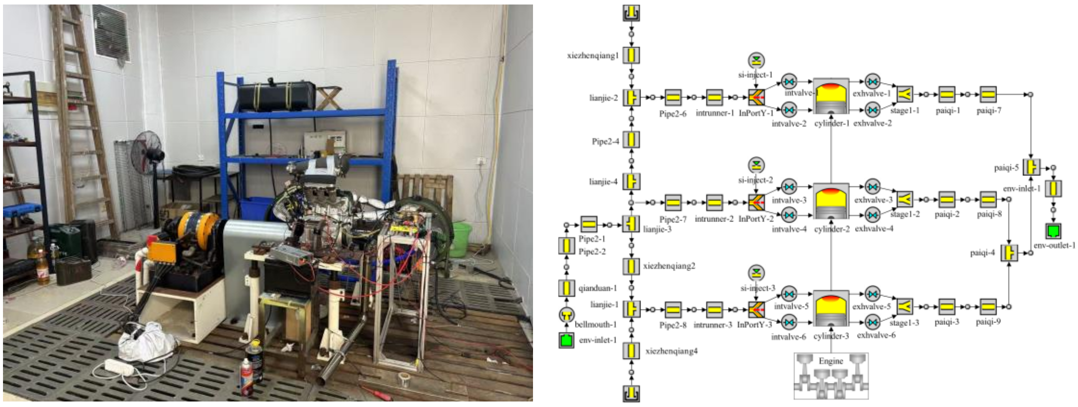

Figure 1. Experimental test bench and one-dimensional simulation model.

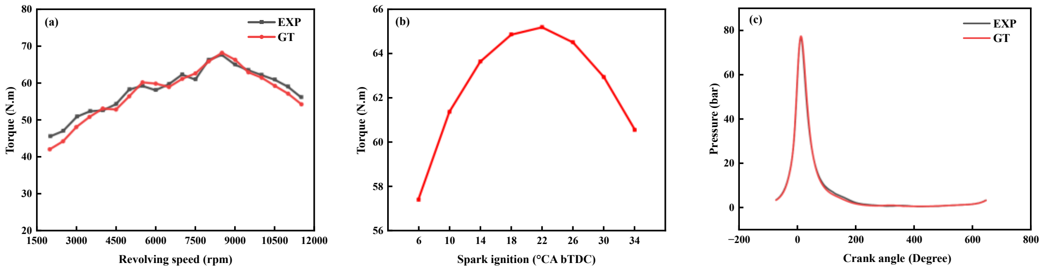

Figure 2. Gasoline engine performance test :(a) external characteristic curve; (b) torque comparison at different ignition advance angles at 8000rpm; (c) validation of cylinder pressure at 8000 rpm: experimental vs GT.

This study employs ANN to construct a cylinder pressure reconstruction model based on the following considerations: First, ANN possesses excellent nonlinear mapping capabilities and can effectively address the multi-parameter coupling characteristics during gasoline engine operation; Second, compared with traditional statistical regression or physics-based reduced-order modeling methods, neural networks do not require pre-setting explicit combustion kinetics equations or detailed chemical reaction mechanisms. They can establish input-output relationships solely through data learning, demonstrating significant advantages when dealing with high-dimensional nonlinear problems [28]. The network topology of ANN consists of three parts: the input layer receives feature variables, the hidden layer extracts deep features through multi-layer nonlinear transformations, and the output layer generates prediction results. Specifically, each neuron performs weighted summation operations, followed by the introduction of nonlinearity through an activation function. The model training process iteratively updates network parameters through a backpropagation algorithm, minimizing the loss function between predicted and actual values. After training completion, the model possesses the capability to predict operating conditions outside the training set, thereby achieving cylinder pressure reconstruction under unmeasured conditions.

The neural network architecture used in this study is shown in Figure 3(a), consisting of an input layer representing crank angle (CA) and operating parameters, and an output layer predicting cylinder pressure or HRR. This neural network structure can approximately capture the complex nonlinear mapping relationship between gasoline engine operating conditions and combustion-related parameters. This study employs two methods for cylinder pressure reconstruction, as shown in Figure 3(b). Method 1's operating parameters include SA and in-cylinder pressure, while fuel injection quantity and engine speed are treated as constant conditions, with the output being training and prediction results of cylinder pressure data. On this basis, a single-zone thermodynamic model is used to differentiate the cylinder pressure data to obtain heat release rate data for all stages from intake to exhaust, including both combustion and non-combustion periods. Method 2's operating

Preprints.org (www.preprints.org) | NOT PEER-REVIEWED | Posted: 16 March 2026 doi:10.20944/preprints202603.1219.v1

parameters include spark advance angle and heat release rate, with the output being training and prediction results of heat release rate data. After obtaining all heat release rate data, using the in-cylinder pressure at intake valve closure as the initial condition, a single-zone thermodynamic model is employed to integrate the heat release rate, thereby reconstructing the cylinder pressure variation with crank angle covering the entire compression, combustion, expansion, and gas exchange processes. This method is based on simplified assumptions including spatial homogeneity of the in-cylinder mixture, ideal gas properties, constant specific heat ratio, and neglect of heat transfer and leakage losses. Although these conditions have certain limitations, they establish a clear mathematical relationship between HRR and cylinder pressure, making it possible to inversely determine in-cylinder pressure through the energy release process.

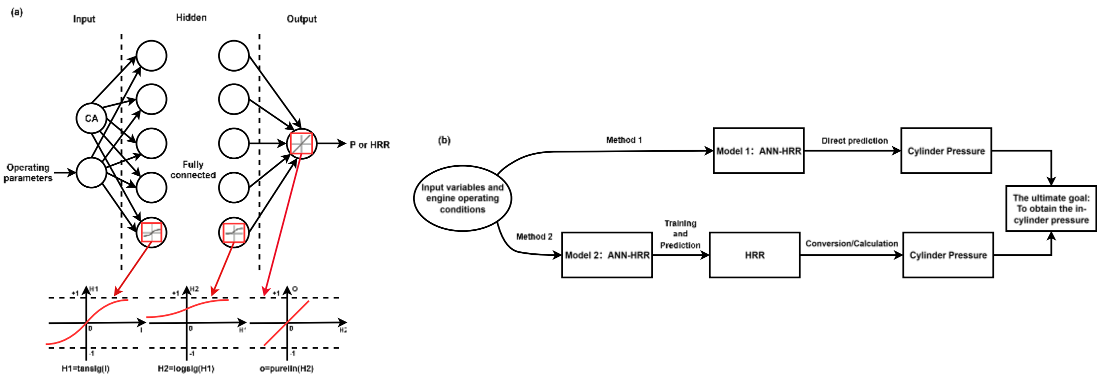

Figure 3. Method for reconstructing in-cylinder pressure under unmeasured conditions based on artificial neural network: (a) network structure; (b) 2 reconstruction strategies.

R Regarding dataset construction, this study employed data covering a complete 720°CA thermodynamic cycle with a sampling interval of 0.1°CA, resulting in 7,200 data points per operating condition. The experiment selected seven different spark advance (SA) conditions (-34°, -30°, -26°, -18°, -14°, -10°, and -6°) as the training basis, totaling 50,400 samples; the -22°CA condition was designated as an independent test set (7,200 samples) to evaluate model generalization capability. During training, a standard resampling strategy partitioned the data as follows: 70% for weight updates, 15% as an internal validation set for monitoring overfitting and triggering the Early Stopping mechanism, and the remaining 15% for internal testing. Methods 1 and 2 employed consistent data partitioning logic, with the distinction that Method 2 used HRR as the target output for training and validation.

This study employed supervised learning methods based on backpropagation algorithms to train the neural network model. During training, network weights and biases were iteratively optimized such that the RMSE between model outputs and experimental data progressively converged to its minimum. To avoid training bias caused by inconsistent variable dimensions, all input and output data were mapped to the [0,1] interval using min-max normalization prior to training; after model training completion, inverse mapping was performed to restore actual physical quantities. Regarding training parameter settings, the maximum number of iterations was set to 1000, the target error to 1×10^{-6}, and the learning rate to 0.01. This parameter configuration achieved a reasonable balance between prediction accuracy and computational cost. Through systematic parameter optimization, the optimal network architecture was determined: dual hidden layers, each containing 5 neurons. In both reconstruction methods proposed in this paper, this topology demonstrated good generalization performance, and prediction effectiveness was unaffected by changes in output targets (in-cylinder pressure or heat release rate). Overall, this network structure achieved satisfactory comprehensive performance in prediction accuracy, convergence stability, and computational efficiency. Regarding activation functions, the first hidden layer employed the hyperbolic tangent function, the second hidden layer employed the logistic function, and the output layer used a linear function to accommodate the requirements of continuous regression tasks.

 doi:10.20944/preprints202603.1219.v1

This study employed RMSE and coefficient of determination (R^2) to quantitatively assess artificial neural network model performance, with specific definitions provided in Equations (1) and (2). RMSE measures the deviation between model output and measured signals; values closer to 0 indicate better agreement between predictions and actual data. R^2 reflects the degree to which the model fits the experimental data variation pattern, with a range of 0 to 1; when R^2 approaches 1, it indicates ideal model fitting. Beyond numerical indicators, this study further compared neural network-predicted cylinder pressure curves and HRR curves with experimental results. This approach not only intuitively displays reconstruction accuracy but also helps verify the physical credibility of prediction results in describing combustion mechanisms. The significance of cylinder pressure reconstruction lies not only in error reduction but more importantly in obtaining combustion characteristic curves with engineering interpretive value; therefore, comparative analysis of curve morphology is indispensable. Through this comprehensive evaluation system, the performance merits and limitations of the two pressure reconstruction strategies proposed in this paper can be systematically compared.

$$RMSE = \sqrt{\frac{1}{n}\sum_{i=1}^{n}\left(y_i - \hat{y}_i\right)^2} \tag{1}$$

$$R^2 = 1 - \frac{\sum_{i=1}^{n}\left(y_i - \hat{y}_i\right)^2}{\sum_{i=1}^{n}\left(y_i - \bar{y}\right)^2} \tag{2}$$

where n is the number of samples, y_i is the i-th measured value, $\hat{y}_i$ is the i-th predicted value, and $\bar{y}$ is the mean of the true values.

3. Results and Discussion

This chapter focuses on exploring the effectiveness of reconstructing in-cylinder pressure using machine learning techniques under predictive operating conditions, specifically when the spark advance angle is -22°CA. It verifies whether the ML framework has the capability to accurately reproduce the in-cylinder pressure curve under such predictive conditions, thereby confirming its feasibility for combustion analysis. This study established two methods for in-cylinder pressure reconstruction: the first is a direct prediction method based on ANN-P; the second is an indirect prediction method based on a full-cycle HRR model (ANN-HRR). To ensure fairness and validity of comparison, both schemes employed optimized artificial neural network models. The result evaluation process adopted a multi-level validation strategy consisting of three progressive stages: first, by calculating quantitative evaluation indices such as RMSE and coefficient of determination (R^2), the overall predictive performance of the models is quantitatively assessed; second, the in-cylinder pressure curves and HRR curves reconstructed by the models are compared and analyzed with experimental measured data to intuitively demonstrate the degree of agreement between prediction results and actual operating conditions; finally, accuracy verification of key performance parameters—IMEP and combustion characteristic points (CA10, CA50, CA90)—between measured and predicted values is conducted, thereby comprehensively evaluating the reliability and applicability of both methods and clarifying their respective advantages and limitations.

3.1. Performance of Method 1 (ANN-P) for Pressure Curve Reconstruction

Figures 4-6 demonstrate the effectiveness of Method 1 (ANN-P) in reconstructing in-cylinder pressure under both measured and unmeasured operating conditions. Figure 4 presents the performance of the in-cylinder pressure prediction model based on ANN-P. The residual histogram uses a black dashed line above zero as a boundary; symmetric distribution on both sides indicates good model performance, while asymmetry indicates poor performance. Residual analysis shows that residuals of both the training set and validation set exhibit approximately normal distribution characteristics centered at zero, with residuals mainly distributed within the range of ±0.4 bar,

Preprints.org (www.preprints.org) | NOT PEER-REVIEWED | Posted: 16 March 2026 doi:10.20944/preprints202603.1219.v1

indicating that model prediction has no systematic bias. The R^2 values on both training and validation sets exceed 0.99, with RMSE values of approximately 0.11 bar and 0.123 bar, respectively. The normal distribution characteristics of residuals indicate that prediction errors primarily originate from random factors, and the model has sufficiently captured the main patterns in the data. Therefore, the established ANN-P model can accurately predict in-cylinder pressure and meets the requirements of practical engineering applications.

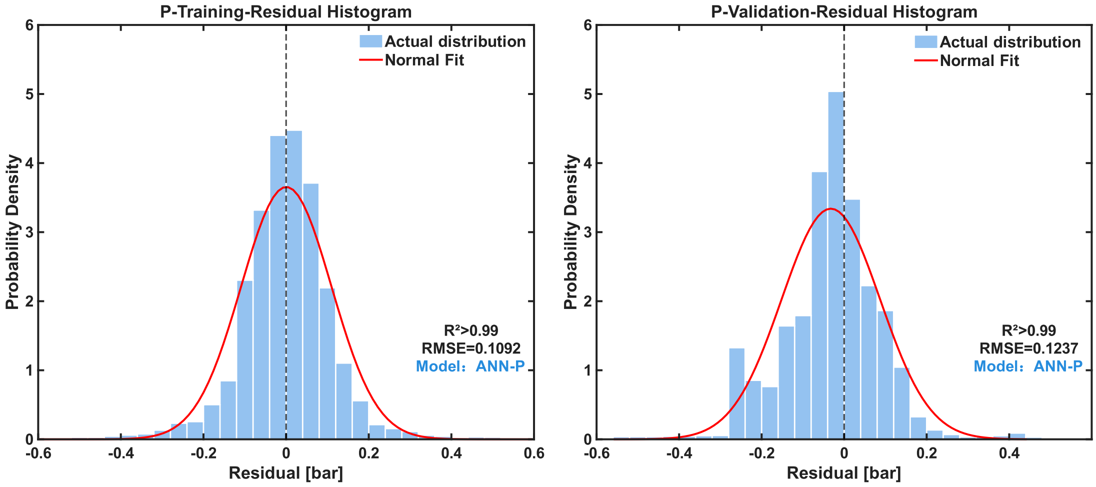

Figure 4. Histogram of residual distribution of ANN-P model on training set and validation set.

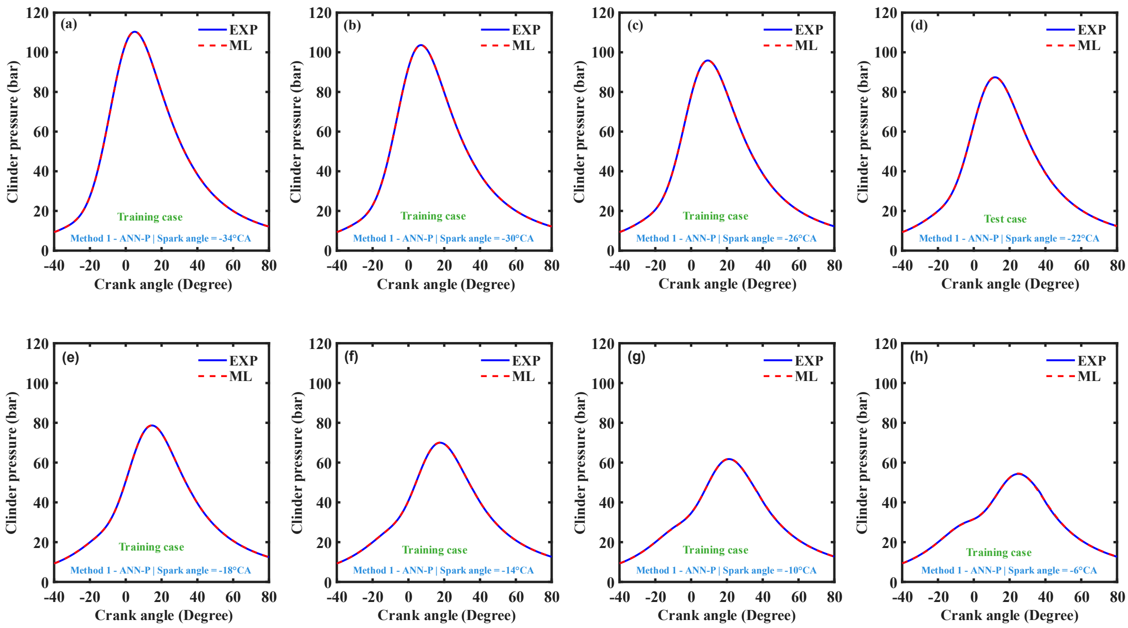

Figure 5. Comparison of measured and predicted in-cylinder pressure values for ANN-P.

Figure 5 shows the comparison between Method 1's in-cylinder pressure prediction results under 8 different spark advance angle conditions and experimental values. Figures (a)-(h) correspond to operating conditions where the spark advance angle gradually retards from -34°CA to -6°CA, with figure (d) representing the test set condition and the remainder being training set conditions. From the overall prediction accuracy perspective, the ML prediction curves and experimental curves show extremely high agreement under all conditions. The rapid pressure rise at the end of the compression stroke, the sharp pressure increase caused by combustion, and the smooth pressure decline during the expansion stroke are all accurately reproduced. The model correctly reflects the influence of ignition timing on in-cylinder pressure: when the spark advance angle retards from -34°CA to -6°CA, peak pressure decreases from approximately 110 bar to about 60 bar, and peak position correspondingly shifts backward—a trend consistent with the thermodynamic characteristics of spark-ignition internal combustion engines. Under early ignition conditions, despite severe pressure gradient changes, the prediction curve can still accurately track experimental values; under late ignition conditions, the characteristic of peak pressure reduction caused by backward shift of combustion phase is equally accurately captured. Notably, the prediction accuracy of the test set condition (figure (d)) is comparable to that of the training set, fully validating the model's excellent generalization capability. This method can accurately reproduce pressure curves at different ignition timings, providing an effective technical means for in-cylinder pressure reconstruction of gasoline engines.

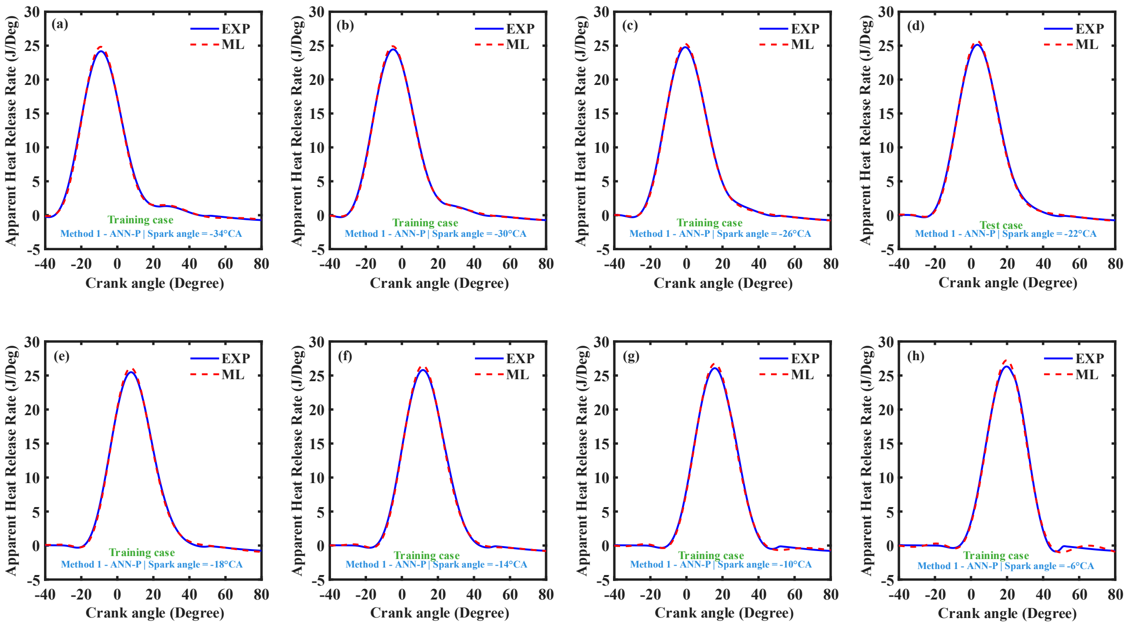

Figure 6. Comparison of actual and predicted heat release rate for ANN-P performance.

Figure 6 shows the comparison between predicted and experimental HRR curves of Method 1 under corresponding operating conditions to further evaluate the combustion characteristics reconstructed by this method. Overall, the model adequately presents the evolution process of the three traditional HRR stages (flame development period, rapid combustion period, and late combustion period), and the predicted curve shows good agreement with the experimental curve. However, during the rapid combustion period, the ML predicted value is slightly higher than the experimental value, with a deviation of approximately 1-2 J/deg in peak HRR, consistent with the minor differences mentioned in pressure prediction. This phenomenon occurs because HRR is derived from the derivative of in-cylinder pressure with respect to crankshaft angle [29]. The HRR value is extremely sensitive to small pressure changes; even small pressure errors are amplified during the derivative process. During the flame development period and late combustion period, both magnitude and phase of HRR reach acceptable accuracy, indicating that pressure phase is well captured. Furthermore, as spark advance angle retards from -34°CA to -6°CA, HRR peak position shifts correspondingly from approximately 10°CA to approximately 30°CA, while peak magnitude remains in the range of 25-28 J/deg. Notably, negative HRR values exist before combustion onset and after combustion completion, attributed to inherent noise characteristics of the original data and the inability of the linear output layer function to provide physical boundary constraints. The prediction accuracy of the test set operating condition (Figure (d)) is comparable to the training set, validating the model's generalization capability. In summary, Method 1 can effectively reconstruct in-cylinder pressure and accurately predict the overall HRR trend.

 doi:10.20944/preprints202603.1219.v1

The result analysis of Method 1 indicates that although it performs well in reproducing the in-cylinder pressure curve, there is a certain deficiency in the accuracy of HRR prediction. The main reason for this is that HRR is derived from the derivative of the in-cylinder pressure, so even a small prediction error in the in-cylinder pressure will be magnified.

3.2. Performance of Method 2 (ANN-HRR) Based on Heat Release Rate

To explore the feasibility of inverting the cylinder pressure from HRR, a second method is introduced. This method uses the HRR experimental data from eight operating conditions as the training and validation sets for ML. Since HRR reflects the detailed combustion process, directly predicting HRR can more reliably capture the combustion stage and intensity. Subsequently, the predicted HRR curve can be integrated based on the first law of thermodynamics to obtain the reconstructed pressure curve. The prediction performance of Method 2 (ANN-HRR) is shown in Figures 7-9.

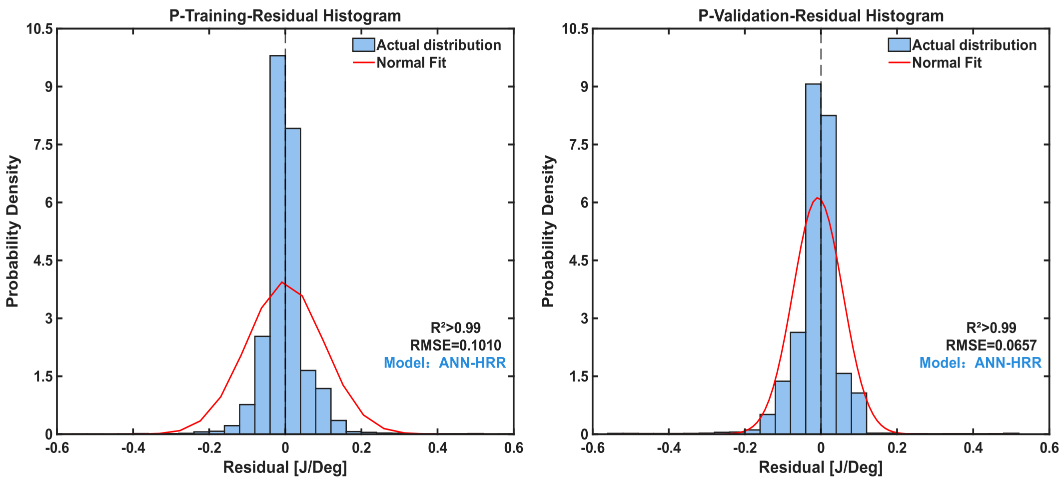

Figure 7. Histogram of residual distribution of ANN-HRR model on training set and validation set.

Figure 7 shows the residual distribution histogram of the established ANN-HRR model on training and validation sets. The figure shows that residuals of both datasets exhibit an approximate normal distribution centered at zero, indicating no systematic bias in model predictions. The coefficient of determination R^2 of the training set exceeds 0.99 with RMSE = 0.1010 J/deg; the validation set R^2 exceeds 0.99 with RMSE = 0.0657 J/deg. The lower RMSE of the validation set compared to the training set indicates good generalization ability without overfitting. Based on the above analysis, the established ANN model has high prediction accuracy and reliability and can accurately predict target parameters.

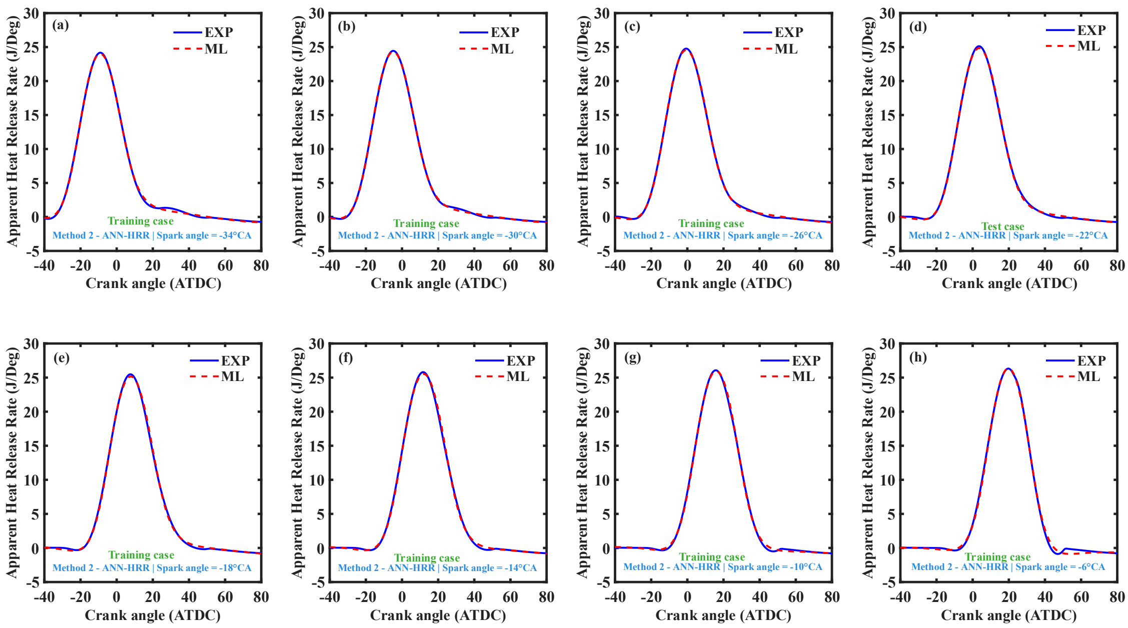

Figure 8. Comparison of actual and predicted values of heat release rate for ANN-HRR performance.

The ANN-HRR-based heat release rate prediction model demonstrates excellent prediction performance under 8 different spark advance angle conditions, as shown in Figure 8. The typical single-peak heat release characteristics of gasoline engine premixed combustion are accurately reproduced: the rapid heat release rise phase starting from the ignition moment, the smooth decline phase after reaching the peak, and the combustion tail all show high agreement with experimental curves. The model correctly captures the influence of ignition timing on combustion phase: when spark advance angle retards from -34°CA to -6°CA, HRR peak position shifts from approximately 5°CA to approximately 25°CA, and peak magnitude decreases from approximately 23 J/deg to approximately 20 J/deg—completely consistent with the combustion physical mechanism of spark-ignition internal combustion engines. Both training and test set conditions show high consistency between predicted curves and experimental values, indicating good model generalization capability. Under retarded ignition conditions, the fit between predicted curve and experimental values in the decline phase shows slight decrease, but overall deviation remains within acceptable range. Additionally, slight negative HRR values before combustion onset and after combustion completion are related to in-cylinder heat transfer losses and raw signal characteristics, with limited impact on overall characterization. In summary, Method 2 can accurately predict transient heat release rate curves under different ignition timings, providing a reliable data foundation for subsequent in-cylinder pressure reconstruction based on HRR.

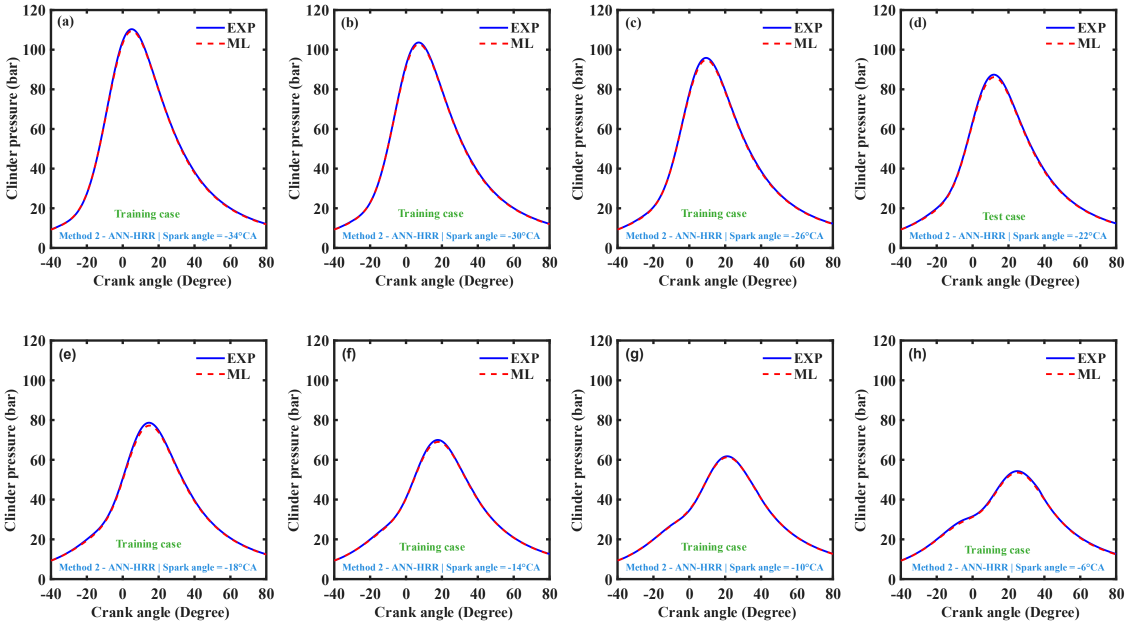

Figure 9. Comparison of measured and predicted in-cylinder pressure values of ANN-HRR.

Based on the above HRR prediction results, in-cylinder pressure reconstructed through thermodynamic first law integration shows high consistency with experimental measurements, as shown in Figure 9. The typical pressure evolution characteristics of the combustion process are accurately reproduced: rapid pressure rise at the end of compression stroke, sharp pressure increase caused by combustion, and smooth pressure decline during expansion stroke all match experimental curves precisely. When spark advance angle retards from -34°CA to -6°CA, peak pressure decreases from approximately 110 bar to about 60 bar, and peak position shifts from approximately 5°CA to about 25°CA—completely consistent with thermodynamic characteristics of spark-ignition internal combustion engines. Under early ignition conditions, although in-cylinder pressure gradient changes dramatically, the prediction curve still accurately tracks experimental values; for retarded ignition conditions, slight underestimation in HRR prediction is effectively smoothed through thermodynamic integration, and prediction errors for both peak pressure and phase are controlled within engineering acceptable range. In summary, Method 2, which predicts heat release rate through ANN-HRR and reconstructs cylinder pressure combined with a single-zone thermodynamic model, demonstrates excellent prediction accuracy and robustness. Compared to Method 1, it achieves more accurate combustion characteristic prediction and provides a reliable technical pathway for gasoline engine combustion diagnosis and control optimization.

3.3. Comprehensive Performance Comparison of the Two Methods

To more comprehensively evaluate the merits of both methods, beyond comparing in-cylinder pressure and combustion heat release rate variations with crankshaft angle as discussed above, further detailed analysis of IMEP and combustion characteristic points (CA10, CA50, CA90) is warranted. By analyzing differences in combustion phase evolution patterns and power output, the inherent mechanisms of performance differences between the two methods are revealed from a thermodynamic perspective.

A comprehensive evaluation and comparison of IMEP and maximum in-cylinder pressure (Pmax) for both prediction methods under different spark advance angle conditions is presented in Figure 10. From Figure 10(a), IMEP exhibits a typical "inverted U-shaped" curve characteristic with respect to spark advance angle, reaching its peak at approximately 22°CA bTDC, corresponding to the maximum brake torque (MBT) region for gasoline engines; when spark advance angle deviates from this optimal interval, IMEP shows a declining trend—consistent with thermodynamic

 doi:10.20944/preprints202603.1219.v1

characteristics of spark-ignition internal combustion engines. From the prediction accuracy perspective, the ANN-P method shows high agreement with experimental values, accurately tracking IMEP variation trend throughout the entire spark advance angle range; the ANN-HRR method exhibits slight underestimation in the intermediate spark advance angle region (14-22°CA bTDC), but still correctly reflects IMEP variation trend with spark advance angle. From Figure 10(b), Pmax exhibits an approximately linear positive correlation with spark advance angle: as spark advance angle increases from 6°CA bTDC to 34°CA bTDC, maximum in-cylinder pressure increases accordingly. This trend is consistent with the physical mechanism of spark-ignition internal combustion engines: earlier ignition results in combustion center of mass closer to top dead center, thereby producing higher peak pressure. Notably, both prediction methods demonstrate excellent accuracy in Pmax prediction, with prediction curves almost completely overlapping experimental values. Comprehensive analysis shows that both methods have comparable prediction accuracy for Pmax; for IMEP prediction, ANN-P method is superior to ANN-HRR method—potentially related to IMEP being an integral parameter over the entire working cycle and thus more sensitive to cumulative errors in HRR prediction; despite these differences, ANN-HRR method can still accurately reflect variation patterns of gasoline engine performance parameters with ignition timing, validating reliability and applicability of this method in predicting gasoline engine combustion characteristics.

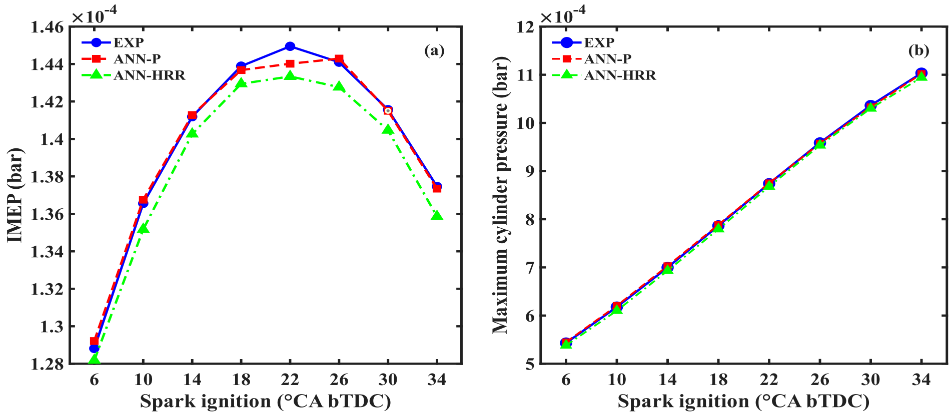

Figure 10. (a) Comparison of IMEP values predicted by ANN-P and ANN-HRR with actual values; (b) Comparison of maximum cylinder pressure predicted by ANN-P and ANN-HRR with actual values.

Figure 11 shows comparison of combustion characteristic points (CA10, CA50, and CA90) obtained from both model methods with actual values. The figure shows that ANN-HRR model demonstrates higher accuracy than ANN-P model in predicting early combustion stage (CA10) and combustion center of mass (CA50), maintaining high consistency between the two regardless of spark advance angle changes, indicating that the model can accurately capture ignition timing influence on the main combustion process and possesses good generalization capability. However, when predicting late combustion stage (CA90), model performance shows significant decline. Considerable deviation exists between predicted and actual values, and error directions of different models are inconsistent under different operating conditions. This may be due to more complex physicochemical processes in late combustion stage, making it difficult for neural networks to precisely fit its nonlinear characteristics. In summary, Method 2 (ANN-HRR) demonstrates extremely high reliability in characterizing early and middle combustion characteristics compared to Method 1 (ANN-P), but both methods have limitations in predicting late combustion characteristics.

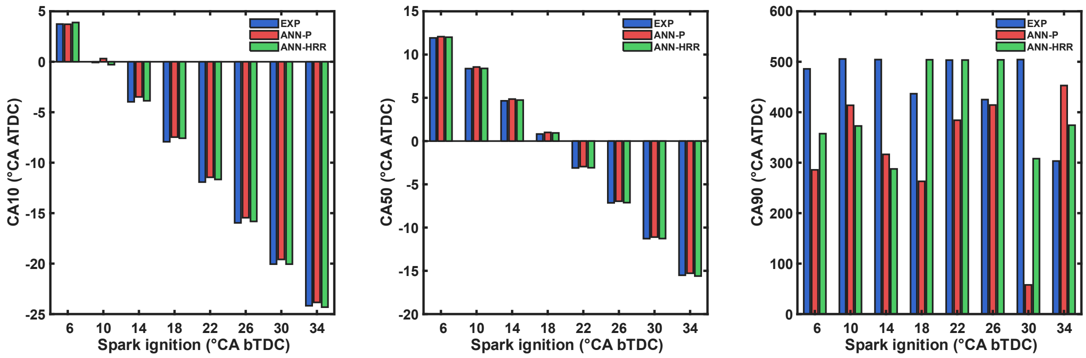

Figure 11. Comparison of actual and predicted values of combustion characteristic points for ANN-P and ANN-HRR.

3.4. Summary of Comparative Results and Limitations

Based on the above analysis, both machine learning-driven in-cylinder pressure reconstruction methods proposed in this study demonstrate good predictive performance. To supplement the above qualitative observations, Table 1 summarizes quantitative predictive performance of both methods under different spark advance angles, and Table 2 summarizes quantitative predictive performance of both methods on IMEP and combustion characteristic points. Consequently, it is further concluded that the ANN-P method shows excellent performance in in-cylinder pressure trajectory reconstruction with high prediction accuracy for IMEP, suitable for applications requiring accurate in-cylinder pressure acquisition such as indicated power calculation and gasoline engine performance calibration; the ANN-HRR method avoids error amplification by directly predicting HRR and is more reliable in characterizing HRR curves and combustion characteristic points, making it suitable for combustion mechanism analysis and combustion phase optimization research. Furthermore, both methods exhibit insufficient prediction accuracy at late combustion phase (CA90), related to complex physicochemical processes in late combustion stage and warranting further optimization and improvement in subsequent studies.

Table 1. R2 and RMSE values of ANN-P and ANN-HRR at different ignition advance angles.

	Method	**-34°**	**-30°**	**-26°**	**-22°**	**-18°**	**-14°**	**-10°**	**-6°**
R^2 (Pressure)	1	1.0000	1.0000	1.0000	0.9999	1.0000	0.9999	0.9999	0.9999
	2	0.9994	0.9997	0.9994	0.9987	0.9991	0.9994	0.9992	0.9997
RMSE（Pressure）	1	0.1099	0.0975	0.0924	0.1237	0.0961	0.1046	0.1136	0.1422
	2	0.5123	0.3281	0.4732	0.6244	0.4744	0.3379	0.3691	0.2178
R^2 (HRR)	1	0.9924	0.9946	0.9959	0.9957	0.9949	0.9939	0.9926	0.9860
	2	0.9998	0.9998	0.9998	0.9998	0.9997	0.9996	0.9993	0.9981
RMSE（HRR）	1	0.3614	0.3087	0.2747	0.2854	0.3131	0.3493	0.3856	0.5534
	2	0.0571	0.0556	0.0574	0.0657	0.0789	0.0859	0.1171	0.1952

Table 2. R2 and RMSE values of ANN-P and ANN-HRR combustion characteristic points and IMEP.

	Method	**CA10**	**CA50**	**CA90**	**IMEP**
R^2	1	0.9965	0.9996	-0.8603	0.99426
	2	0.9998	0.9998	-0.8767	0.99821
RMSE	1	0.5404	0.1706	104.6700	3.82E-07
	2	0.1309	0.0972	105.1300	1.23E-06

4. Summary and Conclusions

In spark-ignition internal combustion engine research, experimental measurement of in-cylinder pressure faces numerous challenges. On one hand, measurement systems require expensive equipment including piezoelectric sensors, crankshaft encoders, signal conditioners, and data acquisition and analysis systems; on the other hand, measurement equipment demands rigorous installation precision and working environment requirements, with complex experimental operations and high maintenance costs. These factors severely restrict widespread application of in-cylinder pressure measurement technology in mass-produced gasoline engines and practical engineering. To overcome these limitations, this study proposes an in-cylinder pressure reconstruction method based on artificial neural networks, achieving accurate in-cylinder pressure prediction through machine learning models and providing an economical and efficient alternative solution for gasoline engine combustion diagnosis. The key conclusions are as follows:

(1) Method 1 (ANN-P) learns in-cylinder pressure variation patterns, with both training and validation sets achieving R^2 exceeding 0.99 and residuals following normal distribution without systematic bias. It can accurately capture pressure evolution throughout compression, combustion, and expansion processes, achieving high-precision IMEP prediction. However, since HRR is obtained through pressure differentiation, small pressure errors during rapid combustion phase are amplified, resulting in deviations in HRR peak region. This method is more suitable for obtaining accurate in-cylinder pressure trajectories and engineering applications for gasoline engine power calibration.

(2) Method 2 (ANN-HRR) directly predicts heat release rate and reconstructs in-cylinder pressure by combining the first law of thermodynamics, avoiding amplification of differentiation errors. The model accurately reproduces premixed combustion characteristics and precisely captures ignition timing regulation of combustion phase, outperforming ANN-P in predicting combustion onset and center of mass location. However, HRR prediction fluctuations in non-combustion regions (especially during compression stroke) produce cumulative effects through integration, causing pressure baseline shift and systematic underestimation of IMEP. This method is more suitable for combustion mechanism analysis, phase optimization, and thermodynamic diagnostic research.

(3) Although both methods perform excellently during main combustion stage, prediction accuracy decreases at late combustion phase (CA90). This is mainly attributed to complex physical and chemical processes involved in late combustion phase, including wall heat transfer, dissociation equilibrium, and unburned hydrocarbon oxidation, which increase model learning difficulty. Future work can further introduce physical constraint layers or combine heat transfer models to improve model generalization capability and prediction accuracy at late combustion phase.

In summary, the two machine learning models established in this study each possess distinct advantages: the ANN-P model is an ideal choice for high-precision pressure reconstruction and power calculation, while the ANN-HRR model provides a reliable tool for in-depth combustion process analysis. This provides important theoretical basis and technical pathway for low-cost, high-performance internal combustion engine development.

Supplementary Materials: The following supporting information can be downloaded at the website of this paper posted on Preprints.org.

Author Contributions: Conceptualization, Y.Z. and X.Z.; methodology, Y.Z. and Q.X.; software, Y.Z. and Q.X.; validation, Y.Z. and Q.X.; formal analysis, Y.Z.; investigation, Y.Z. and Q.X.; resources, Y.Z. and X.Z.; data curation, Y.Z. and Q.X.; writing—original draft preparation, Q.X.; writing—review and editing, Y.Z. and Q.X.; visualization, Y.Z. and Q.X.; supervision, Y.Z. and X.Z.; project administration, Y.Z. and X.Z.; funding acquisition, Y.Z. and X.Z., All authors have read and agreed to the published version of the manuscript.

Funding: This research was funded by the Natural Science of Zhejiang Province (CN) (Grant No. LQ20E060003), the Zhejiang Province Basic Public Welfare Research Project (Grant No. LGG20E050007), the Scientific Research Foundation of Zhejiang University City College (Grant No. X-202205), and the 2021 Teacher Professional Development Program for Domestic Visiting Scholars in universities (Grant No. FX2021105).

Data Availability Statement: The original contributions presented in this study are included in the article. Further inquiries can be directed to the corresponding author.

 doi:10.20944/preprints202603.1219.v1

Conflicts of Interest: The authors declare no conflicts of interest.

Abbreviations

SA	Spark Advance Angles
ANN	Artificial Neural Network
RMSE	Root Mean Square Error
IMEP	Indicated Mean Effective Pressure
HRR	Heat Release Rate
CA10	Crank Angle at 10% Cumulative Heat Release
CA50	Crank Angle at 50% Cumulative Heat Release
CA90	Crank Angle at 90% Cumulative Heat Release
CA	Crank Angle
CFD	Computational Fluid Dynamics
CPU	Central Processing Unit
ML	Machine Learning
MBT	Maximum Brake Torque

References

1. Reitz, R.D.; Ogawa, H.; Payri, R.; et al. The future of the internal combustion engine. Int. J. Engine Res. 2020, 21, 3–10.
2. Leach, F.; Kalghatgi, G.; Stone, R.; et al. The scope for improving the efficiency and environmental impact of internal combustion engines. Transp. Eng. 2020, 1, 100005. https://doi.org/10.1016/j.treng.2020.100005.
3. Sarathy, S.M.; Farooq, A.; et al. Recent progress in gasoline surrogate fuels. Prog. Energy Combust. Sci. 2018, 65, 67–108. https://doi.org/10.1016/j.pecs.2017.09.004.
4. Gainey, B.; Longtin, J.P.; Lawler, B. A Guide to Uncertainty Quantification for Experimental Engine Research and Heat Release Analysis. SAE Int. J. Engines 2019, 12, 509–523. https://doi.org/10.4271/03-12-05-0033.
5. Corti, E.; Forte, F.; et al. Automatic combustion phase calibration with extremum seeking approach. J. Eng. Gas Turbines Power 2014, 136, 1–8.
6. Guardiola, C.; Martín, ; et al. Cycle by cycle NOx model for diesel engine control. Appl. Therm. Eng. 2017, 110, 1011–1020. https://doi.org/10.1016/j.applthermaleng.2016.08.170.
7. Liu, H.F.; et al. Investigation on the potential of high efficiency for internal combustion engines. Energies 2018, 11, 513. https://doi.org/10.3390/en11030513.
8. Teodosio, L.; Bozza, F.; et al. Impact of the laminar flame speed correlation on the results of a quasi-dimensional combustion model for Spark-Ignition engine. Energy Procedia 2018, 148, 631–638. https://doi.org/10.1016/j.egypro.2018.08.151.
9. Zhu, S.P.; Akehurst, A.; et al. A review of the pre-chamber ignition system applied on future low-carbon spark ignition engines. Renew. Sustain. Energy Rev. 2022, 154, 111872.
10. Goldsborough, S.S.; Hochgreb, S.; Vanhove, G.; et al. Advances in Rapid Compression Machine Studies of Low- and Intermediate-Temperature Autoignition Phenomena. Prog. Energy Combust. Sci. 2017, 63, 1–78. https://doi.org/10.1016/j.pecs.2017.05.002.
11. Moser, M.; Pradhan, M.; Emal, I.U.H.; et al. Low-power AlGaN/GaN pressure sensors for harsh environmental conditions with high sensitivity. Power Electron. Devices Components 2025, 10, 100076.
12. Han, X.G.; Huang, M.; Wu, Z.T.; et al. Advances in high-performance MEMS pressure sensors: design, fabrication, and packaging. Microsyst. Nanoeng. 2023, 6, 43–76. https://doi.org/10.1038/s41378-023-00620-1.
13. Kodavasal, J.; Moiz, A.A.; Ameen, M.; et al. Using Machine Learning to Analyze Factors Determining Cycle-to-Cycle Variation in a Spark-Ignited Gasoline Engine. J. Energy Resour. Technol. 2018, 140, 102204. https://doi.org/10.1115/1.4040062.
14. Zhao, L.; Moiz, A.A.; et al. Examining the role of flame topologies and in-cylinder flow fields on cyclic variability in spark-ignited engines using large-eddy simulation. Int. J. Engine Res. 2018, 19, 886–904. https://doi.org/10.1177/1468087417732447.

 doi:10.20944/preprints202603.1219.v1

15. Akgül, V.; Özener, O.; et al. Numerical Investigation and Multi-Objective Optimization of Internal EGR and Post-Injection Strategies on the Combustion, Emission and Performance of a Single Cylinder, Heavy-Duty Diesel Engine. Energies 2021, 14, 15. https://doi.org/10.3390/en14010015.
16. Aliramezani, M.; Koch, ; et al. Modeling, diagnostics, optimization, and control of internal combustion engines via modern machine learning techniques: A review and future directions. Prog. Energy Combust. Sci. 2022, 88, 100967. https://doi.org/10.1016/j.pecs.2021.100967.
17. Ihme, M.; Chung, W.T.; Mishra, A.A. Combustion machine learning: Principles, progress and prospects. Prog. Energy Combust. Sci. 2022, 91, 101010. https://doi.org/10.1016/j.pecs.2022.101010.
18. Bhatt, A.N.; Shrivastava, ; et al. Application of Artificial Neural Network for Internal Combustion Engines: A State of the Art Review. Arch. Compute. Methods Eng. 2022, 29, 1–23. https://doi.org/10.1007/s11831-021-09596-5
19. Solmaz, Ö., Gürbüz, H., and Karacor, M. Comparison of Artificial Neural Network and Fuzzy Logic Approaches for the Prediction of In-Cylinder Pressure in a Spark Ignition Engine. J. Dyn. Syst. Meas. Control 2020, 142, 1–11. https://doi.org/10.1115/1.4047014
20. Y. Ji, C. Yao, E. Song, Y. Ke, X. Yu and J. Xu. Prediction of Diesel Engine Cylinder Pressure Based on SSA-BiLSTM Model. In Proceedings of the 2023 IEEE International Conference on Electrical, Automation and Computer Engineering (ICEACE), Changchun, China, 2023, pp. 327-334. https://doi.org/10.1109/ICEACE60673.2023.10442596
21. Zhang, R., Yu, Y., Ou, S. et al. Engine cylinder pressure reconstruction method with multi-source information fusion. J. Mech. Sci. Technol. 2025, 39, 5025–5035. https://doi.org/10.1007/s12206-025-0811-3
22. Raissi, M.; Perdikaris, P.; et al. Physics-informed neural networks: A deep learning framework for solving forward and inverse problems involving nonlinear partial differential equations. J. Comput. Phys. 2019, 378, 686–707. https://doi.org/10.1016/j.jcp.2018.10.045.
23. Cai, S.Z.; Mao, Z.P.; Wang, Z.C.; et al. Physics-informed neural networks (PINNs) for fluid mechanics: A review. J. Mech. 2021, 37, 1727–1738. https://doi.org/10.1007/s10409-021-01148-1.
24. Owoyele, O.; Pal, P.; Vidal Torreira, A.; et al. Application of an automated machine learning-genetic algorithm (AutoML-GA) coupled with computational fluid dynamics simulations for rapid engine design optimization. Int. J. Engine Res. 2022, 23, 1586–1601. https://doi.org/10.1177/14680874211023466
25. Turkson, R.F.; et al. Artificial neural network applications in the calibration of spark-ignition engines: An overview. Eng. Sci. Technol. Int. J. 2016, 19, 1346–1359. https://doi.org/10.1016/j.jestch.2016.03.003
26. Badra, J.A.; Khaled, F.; Tang, M.; et al. Engine Combustion System Optimization Using Computational Fluid Dynamics and Machine Learning: A Methodological Approach. J. Energy Resour. Technol. 2021, 143, 022306. https://doi.org/10.1115/1.4047978.
27. Huang, Q.; Xie, T.F.; Liu, J.L. Machine Learning-Assisted Reconstruction of In-Cylinder Pressure in Internal Combustion Engines Under Unmeasured Operating Conditions. Energies 2025, 18, 5235. https://doi.org/10.3390/en18195235.
28. Zhang, C.; Guo, Y.; Liu, M. A review of the development and applications of artificial neural network models. Comput. Eng. Appl. 2021, 57, 57–69.
29. Mohan, B.; Badra, J. An automated machine learning framework for piston engine optimization. Appl. Energy Combust. Sci. 2023, 13, 100106. https://doi.org/10.1016/j.jaecs.2022.100106.